RAPID RESEARCH LETTER

pssrrl
physica status solidi
www.pss-rapid.com

Stretch/Compress-Modulated Spin Splitting in One-Dimensional Melem Chain with a Helical Structure

Dong Han, Xue-Jiao Chen, Hai Xu, Chen Jiao, Ji-Lian Xu, Ke-Xue Li, Lei Liu,* Yao-Biao Li,* and De-Zhen Shen*

It is demonstrated that spin splitting can be induced and further modulated in a one-dimensional (1D) helical melem chain with a helical structure by first-principles calculations. The spin splitting occurs at the charge-localized states at valence band due to the breaking of inversion symmetry by the helical structure. The maximum spin-split energy reaches 0.81 meV, without any heavy elements in the melem chain. The helical melem chain is facile to stretch or compress, as a molecule spring with a spring constant of $1.04\,\text{N m}^{-1}$, leading to the spin-split energy effectively varying from 0.81 (196 GHz) to 0.04 meV (10 GHz) along with the periodic lattice changing from 4.0 to 15.0 Å. These results exhibit a unique mechanism for driving the spin splitting in 1D materials, in particular for those helical big molecules, and that in fact offers an original way to not only design the regulatable 1D components in the fields of spintronics but also measure the helix of molecule chains by resonating with microwave frequency.

Spin energy splitting, as a fundamental concept in condensed matter, now has attracted significant interests. This unique phenomenon can be used to create and further manipulate the spin degrees of freedom in solid-state systems, aiming to the spintronic devices.[1] With the Dresselhaus[2] and Rashba[3] spin–orbit coupling (SOC) effect, one of the essential factors leading to the spin splitting in a nonmagnetic solid-state system is to break its inversion symmetry.[3] The breaking of inversion symmetry can intrinsically exist in 3D crystals[4] or be induced externally in 2D structures.[5,6] For a one-dimensional (1D) system, the inversion symmetry breaking is mostly carried out through the latter case. The inversion symmetry in 1D system is broken at the interface of quantum wire[7] or by inducing the electric field perpendicular to the wire's axis.[8,9] However, the intrinsic inversion symmetry

breaking in the 1D system, leading to the spin-split effect, is still not well understood.

Recently, the 1D screw dislocation with the SOC effect in the semiconductors is theoretically predicted to generate the spin-split defect states.[10] The spin texture of those spin-polarized defect states, only pertaining to the inherent symmetry of screw dislocation, is obviously different from that of spin-polarized states from the conventional Rashba and Dresselhaus effect. The similar mechanism was also found in chiral carbon nanotubes[11] and the carbon nanotubes wrapped with DNA molecules.[12] Actually, the simple helical structure in the 1D system naturally possesses the structural inversion asymmetry. In the 1D helical structure, the configuration in any plane perpendicular to helix axis has no central symmetry. Therefore, the 1D helical structure is an excellent case for studying the spin-split effect in the 1D system.

Although the twisted van der Waals GeS nanowire is successfully synthesized recently,[13] the natural molecules, compared with those semiconductors and nanotubes, are more facile to experimentally synthesize into the unique helical structure along the specific axis. In the current case, the 1D helical nanostructure could be artificially constructed by means of self-assembly of molecular units. The melem $(C_6N_7(NH_2)_3)$ is this kind of common molecular unit by connecting via tertiary amines, to form a large-area carbon nanosheet for the application of metal-free photocatalyst.[14] Once the tertiary amines link the melem units in a different plane, it can construct the spatially complicated superstructures. For example, by treating the melem molecules in boiling water, the melem molecules are rearranged and successfully assemble the 1D helical structure.[15]

In this letter, from the first-principles calculation based on density functional theory (DFT) with SOC, the mechanical and electronic properties of 1D melem chain with a helical structure are investigated. Here, we demonstrated that the mesoscopic helical structure can induce the obvious spin splitting at a valence band (VB), but no spin splitting of a conduction band (CB) in the band structure. This spin splitting originates from the gradient of potential in the xy plane induced by a helical structure along the z direction. This 1D helical structure built from the melem molecules is very facile to stretch or compress as a spring. The spring constant is deduced to be $1.04\,\text{N m}^{-1}$. More importantly, the magnitude of split energy can be

Dr. D. Han, Dr. X.-J. Chen, Prof. H. Xu, Dr. C. Jiao, Dr. J.-L. Xu, Dr. K.-X. Li, Prof. L. Liu, Prof. Y.-B. Li, Prof. D.-Z. Shen
State Key Laboratory of Luminescence and Applications
Changchun Institute of Optics, Fine Mechanics and Physics
Chinese Academy of Sciences
Changchun 130033, P. R. China
E-mail: liulei@ciomp.ac.cn; liyaobiao@ciomp.ac.cn; shendz@ciomp.ac.cn

Dr. X.-J. Chen, Dr. C. Jiao
University of Chinese Academy of Sciences
Beijing 100049, P. R. China

effectively regulated by stretching or compressing the helical chain. When the periodic lattice increases from 4.0 to 15.0 Å, the split energy can vary from 0.81 to 0.04 meV even if no heavy elements exist in the melem molecules, corresponding to the microwave frequency from 10 (0.04 meV) to 196 GHz (0.81 meV). Our results offer an original way to design the regulatable 1D components in the spintronic devices and propose a new method to measure the helix of molecule chains.

As the building blocks, melem molecules can be used to assemble various kinds of C_3N_4 polymers. For example, the most stable form is the graphitic $C_3N_4(g-C_3N4)$, where the melem units are connected via the tertiary groups in the graphitic planes. This g-C_3N_4 exhibits an excellent thermal stability and a semiconducting behavior, showing as a potential candidate for metal-free polymeric photocatalysts.[14,16] In here, we constructed a model of the connected melem molecules with a helical structure as shown in **Figure 1**b,c. From the side view, the melem molecules are constructed to a 1D chain with a left-handed helical surface in the axis direction (named as the z direction) via connecting at the amino groups, looking as an Archimedean's screw. From the top view, every three melem molecules can rotate one circle. At the same time, the melem molecule would lift a certain distance up along the z direction, which is periodic lattice $z(L_z)$. Figure 1c shows that the L_z can gradually vary from 4.0 Å to a very large value 15.0 Å without bonds breaking. But from Figure 1b, compared with $L_z = 4.0$ Å, the in-plane triangle significantly shrinks

when $L_z = 15.0$ Å. This 1D helical melem chain can be stretched or compressed, regarding as a mechanical spring. Therefore, to understand the mechanical property of this spring, we calculated that the total energy of the spring system varies along with L_z changes, as shown in Figure 1a. We found that the total energy gently changes from 4.0 to 15.0 Å, with the minimum value at 9.5 Å. The total energy is only 0.90 eV for 4.0 Å and 1.12 eV for 15.0 Å higher than the minimum value, respectively. This amount of energy increasing can be attributed to the global structural distortion, rather than the bond length between C and N varying. However, the total energy remarkably increases when $L_z < 4.0$ Å. Since the interlayer distance of g-C_3N_4 is about 3.3 Å,[17] this sharp increase in the total energy can be derived from the strong interlayer interaction. Moreover, we also deduced the spring constant k based on the Hooke's law $W = \frac{k}{2}x^2$, where W is the spring potential energy and x is the distance of stretching or compressing the spring. The spring constant is about 0.065 eV Å^{-2}, i.e., 1.04 N m^{-1}, which is comparable with that of helicenes,[18] and 1000-times smaller than that of chemical bonds. Therefore, the excellent mechanical property of the 1D helical melem chain with easy stretching/compressing in a large range indicates a large regulating range on its electronic properties.

First, we calculated the band structure of helical melem chain without SOC. As shown in **Figure 2**a, the helical melem chain exhibits an indirect-band character with an energy gap of about 2 eV. The VB in the band structure is very flat, compared with the large dispersion of CB. Therefore, the electron transition between VB and CB can occur for absorbing or emitting photons. The charge density distribution in Figure 2b offers a clear physical picture in the band structure. The charge density of VB is strongly localized around the N ions at the inner space, but
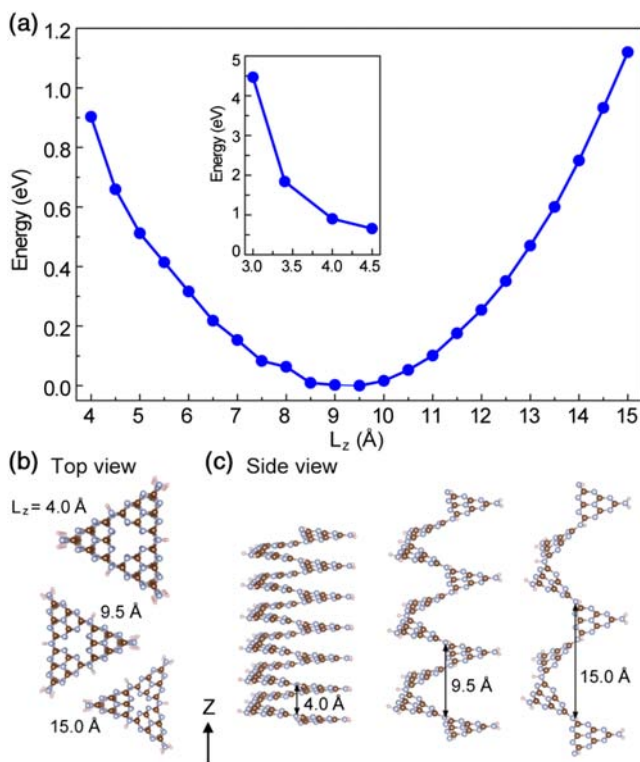

Figure 1. a) The calculated energy as a function of lattice Z, L_z. The inset is the calculated energy changes along with L_z varying from 3.0 to 4.5 Å. The minimum energy is set to 0 eV when $L_z = 9.5$ Å. b) Top view and c) side view of atomic structures of 1D helical melem chain. Brown, blue, and light pink spheres represent C, N, and H atoms.
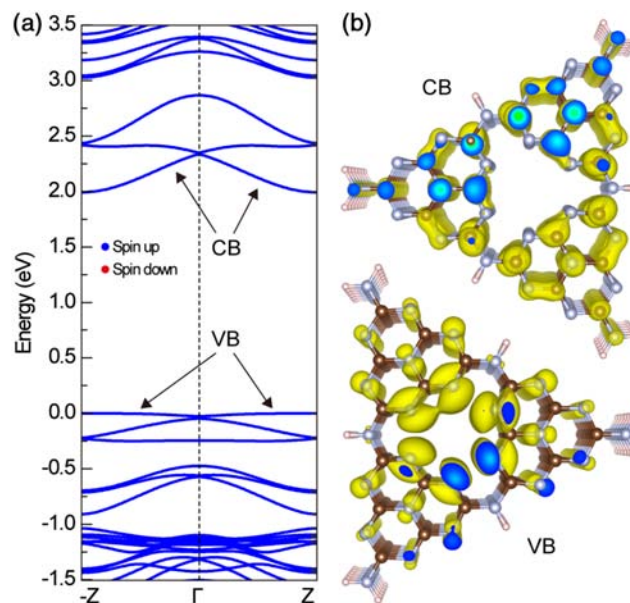

Figure 2. a) Band structure of the 1D helical melem chain with $L_z = 4.0$ Å. b) Top view of charge density distributions of CB and VB as shown with black arrows. The valance band maximum is set to 0 eV. The yellow isosurface is 0.002 e Å^{-3}. The blue part is a result of cutting the charge density at the periodic boundary.

the charge of CB is delocalized at the helical C–N plane. Those advanced electronic characters, including the appropriate bandgap and the obvious charge separation in space between VB and CB, are suitable for photocatalyzed splitting of water. Those characters are partially derived from melem trimers, e.g., the three melem molecules-built in-plane structure. For example, as shown in Figure S1, Supporting Information, the energy gap between highest occupied molecular orbital (HOMO) and lowest unoccupied molecular orbital (LUMO) levels is about 2.07 eV, which determines the bandgap of the 1D helical melem chain. The HOMO level is doubly degenerate with the complementary charge distributions, strongly localizing around the N ions at the inner triangular space, whereas the LUMO level is also doubly degenerate with the complementary charge distributions, delocalizing at the C–N plane.

With no doubt, the helical structure can affect its electronic properties significantly. To distinguish the helical structure-induced effect in the band structure, the band structures of the helical melem chain and the stacking melem trimers are compared in Figure S2, Supporting Information. Remarkable differences in their band structures are found. For the stacking melem trimers, its band structure looks like the combination of energy levels of melem trimers with a weak interaction. The states are becoming flat due to the vanished interaction of those states, when the interlayer distance is changing from 4.0 to 6.5 Å. This is because those melem trimers are separate in space and the charge distributions of the states are localized around the discrete melem trimers. Moreover, the double degeneracy of HOMO and LUMO levels is almost preserved in the VB and CB. But for the helical melem chain, the energy states are dispersed largely and crossing at the center and edge of the Brillouin zone, indicating that the distinctive band structure is due to the helical structure. The energy states keep a large dispersion when L_z changes from 4.0 to 6.5 Å, especially to the localized-charge VB. This is because the increase of L_z dominantly leads to the distortion of the helical structure, rather than separating the melem molecules. The melem molecules are still linked even if the L_z increases greatly. As a result, the interaction between the states is still strong. For the VB when $L_z = 6.5$ Å, the localized charge distribution at the inner space will form a charge chain in space for carrier's transport under the distorted helical structure, making the energy dispersion larger. Moreover, the doubly degenerated VB and CB, which are derived from melem trimers, are reduced at the helical melem chain.

More importantly, the helical structure of the 1D melem chain would break the inversion symmetry in the z direction, leading to a spin splitting in the band structure. As shown in **Figure 3**, without SOC, the VB shows the spin degeneracy in all Brillouin zone. Once SOC is considered, it is found that the VB only keep its spin degeneracy at G and Z points of the Brillouin zone, while the spin degeneracy is clearly lifted in the range between G and Z. This spin degeneracy at the high symmetry points while spin splitting in between demonstrates that the inversion symmetry is broken in the 1D melem chain by the helical structure, rather than breaking the time reversal symmetry.[19] The spin texture of the lifted spin electron states in the Brillouin zone is also an important feature, which can be used to determine the contributions of Dresselhaus effect and Rashba effect.[20,21] In our case, however, the wave vector can only vary in 1D direction,
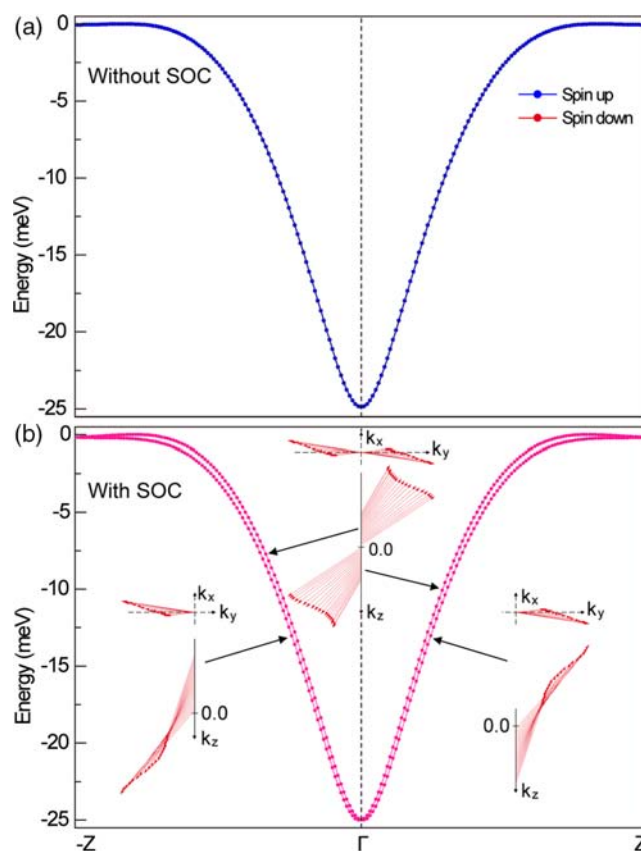

Figure 3. The band structures of VB a) without SOC and b) with SOC. The VBM is set to 0 eV. Red arrows in the inset of (b) indicate the orientation of spins in the corresponding split bands.

the spin texture of the lifted spin states can be classified into neither Dresselhaus effect nor Rashba effect. As shown in Figure 3b, for upper lifted VB, the arrows of spin orientation principally point to the negative k_z direction when the wave vector $k_z < 0$, while the arrows of spin orientation point to the positive k_z direction when the wave vector $k_z > 0$. There are some k_x and k_y components of spin orientation, resulting from a certain rotation of the gradient of the potential α_{xy} in different $k_x - k_y$ planes. But the larger the magnitude of wave vector k_z is, the more the k_z component of spin orientation is, combining with the less the k_x and k_y components of spin orientation are. The arrows of spin orientation for the lower lifted spin state is rightly opposite to that of the upper lifted spin state. This spin texture distinctly indicates the effective spin splitting in VB. In Figure S3, Supporting Information, it is clearly found that the spin splitting only occurs in VB, rather than CB. This is because the charge of VB is strongly localized around N atoms in the inner triangular space, leading to the spin of VB electron can effectively interact with the sp^2 hybrid orbitals of N. But for the charge of CB delocalized at the C–N plane, the SOC between the spin of CB electron and the p orbitals of C or N barely happens.

Since the melem chain can be easy to stretch or compress in a large range, it really concerns that how the mechanical operation affects the spin splitting in its electronic properties. To answer this question, we have calculated the spin-split energy changes
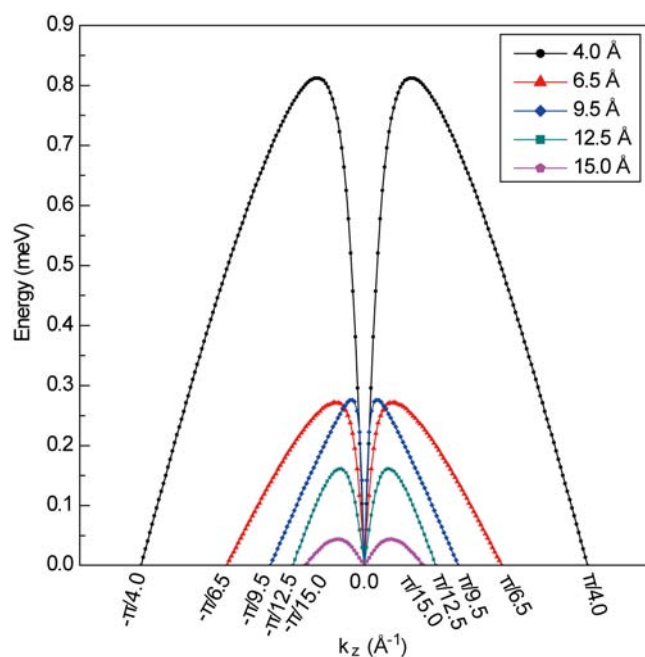
**ADVANCED
SCIENCE NEWS**

www.advancedsciencenews.com

physica **pss** rrl
status solidi

www.pss-rapid.com

Figure 4. The spin-split energy in the 1D helical melem chain with various L_z as a function of k_z-vector.

along with the L_z varies, as shown in **Figure 4**. It is clearly found that, along with the L_z of melem chain stretches from 4.0 to 15.0 Å, the spin-split energy decreases from 0.81 to 0.04 meV. Note that, the split energy is reasonable, because the melem chain contains no heavy elements. However, the split energy does not decrease gradually. The split energy sharply drops by 0.54 meV from $L_z = 4.0$ to 6.5 Å. But for $L_z > 6.5$ Å, the split energy only decreases by 0.23 meV from $L_z = 6.5$ to 15.0 Å. Moreover, the split energy for $L_z = 9.5$ Å is reversely larger than that for $L_z = 6.5$ Å. This is not a special case. The calculated spitting energy for $L_z = 3.4$ Å is also smaller than that for $L_z = 4.0$ Å, which is very similar to the case between $L_z = 9.5$ and 6.5 Å. Therefore, we concluded that the controllable helical structure not only directly modulates the spin-split energy but also includes an influence as a perturbation though affecting its band structure.

The spin-split energy in the 1D helical melem chain can match and therefore resonate with the electromagnetic field in the microwave band from 10 GHz (0.04 meV) to 196 GHz (0.81 meV). Stretch/compress the chain can effectively modulate the resonant frequency from 10 to 196 GHz. Accordingly, the resonant frequency can be regarded as the signature of the helix of molecule chains, proposing a new method to measure the helical structures of molecule chains. In our case, from its band structure, the 1D helical melem chain is a semiconductor, e. g., the VB is fully occupied. There is no empty state for electron's transition between the spin-split states in VB. Therefore, to realize the resonate with microwave for electron's transition between the split states, the Fermi level should be shifted below the valence band maximum (VBM) first. This can be achieved by external doping[22,23] or controlled by the external electric field to further realize the on/off the microwave resonation.

In summary, we have shown that the helical structure could induce an observable spin splitting of VB in the band structure of the 1D helical melem chain. The spin splitting of VB originated from the SOC between localized electron spin of VB and N ions combining with the helical-structure-induced inversion asymmetry. The spin-split energy, without any heavy elements in the melem chain, can reach a maximum value of 0.81 meV. The 1D helical melem chain can be regarded as a molecule spring, which is facile to stretch or compress with the spring constant of 1.04 N m^{-1}. As a result, the spin-split energy can regulate from 0.81 meV for $L_z = 4.0$ Å to 0.04 meV for $L_z = 15.0$ Å, corresponding to the microwave band from 10 GHz (0.04 meV) to 196 GHz (0.81 meV). Our work exhibits a unique mechanism for driving the spin splitting, in which various exciting phenomena may be found in the 1D system.[7,24–26] This offers not only an original way to design the regulatable 1D components in a massive of spintronic applications but also the application on measuring the helix of molecule chains by resonating with microwave.

Supporting Information

Supporting Information is available from the Wiley Online Library or from the author.

Acknowledgements

Conflict of Interest

The authors declare no conflict of interest.

Keywords

[1] I. Žuti, J. Fabian, *Rev. Mod. Phys.* **2004**, 76, 323.
[2] G. Dresselhaus, *Phys. Rev.* **1955**, 100, 580.
[3] E. I. Rashba, *Sov. Phys. Solid State* **1960**, 2, 1109.
[4] X. Zhang, Q. Liu, J. W. Luo, A. J. Freeman, *Nat. Phys.* **2014**, 10, 387.
[5] A. D. Caviglia, M. Gabay, S. Gariglio, N. Reyren, C. Cancellieri, *Phys. Rev. Lett.* **2010**, 104, 126803.
[6] J. H. Dil, F. Meier, J. Lobo-Checa, L. Patthey, G. Bihlmayer, *Phys. Rev. Lett.* **2008**, 101, 266802.

[7] C. H. L. Quay, T. L. Hughes, J. A. Sulpizio, L. N. Pfeiffer, K. W. Baldwin, K. W. West, D. Goldhaber-Gordon, *Nat. Phys.* **2010**, *6*, 336.

[8] D. Liang, X. P. A. Gao, *Nano Lett.* **2012**, *12*, 3263.

[9] S. Zhang, N. Tang, W. Jin, J. Duan, X. He, X. Rong, C. He, L. Zhang, X. Qin, L. Dai, Y. Chen, W. Ge, *Nano Lett.* **2015**, *15*, 1152.

[10] L. Hu, H. Huang, Z. Wang, W. Jiang, X. Ni, Y. Zhou, V. Zielasek, M. G. Lagally, B. Huang, *Phys. Rev. Lett.* **2018**, *121*, 066401.

[11] L. Chico, M. P. López-Sancho, *Phys. Rev. Lett.* **2004**, *93*, 176402.

[12] Y. Perlitz, K. Michaeli, *Phys. Rev. B* **2018**, *98*, 195405.

[13] P. Sutter, S. Wimer, E. Sutter, *Nature* **2019**, *570*, 354.

[14] X. Wang, K. Maeda, A. Thomas, K. Takanabe, G. Xin, J. M. Carlsson, K. Domen, *Nat. Mater.* **2008**, *8*, 76.

[15] M. J. Shipia, K. Pia, S. Wolfgang, *Chem. Eur. J.* **2012**, *18*, 3248.

[16] W. J. Ong, L. L. Tan, Y. H. Ng, S. T. Yong, *Chem. Rev.* **2016**, *116*, 7159.

[17] J. E. Lowther, *Phys. Rev. B* **1999**, *59*, 11683.

[18] M. Jalaie, S. Weatherhead, K. B. Lipkowitz, *Electron. J. Theor. Chem.* **1997**, *2*, 268.

[19] M. Kepenekian, R. Robles, C. Katan, D. Sapori, L. Pedesseau, *ACS Nano* **2015**, *9*, 11557.

[20] S. D. Ganichev, V. V. Bel'kov, L. E. Golub, E. L. Ivchenko, P. Schneider, S. Giglberger, J. Eroms, J. De Boeck, G. Borghs, W. Wegscheider, D. Weiss, *Phys. Rev. Lett.* **2004**, *92*, 256601.

[21] L. Meier, G. Salis, I. Shorubalko, E. Gini, S. Schön, *Nat. Phys.* **2007**, *3*, 650.

[22] D. Wang, D. Han, X. B. Li, S. Y. Xie, N. K. Chen, W. Q. Tian, D. West, H. B. Sun, *Phys. Rev. Lett.* **2015**, *114*, 196801.

[23] D. Wang, D. Han, D. West, N. K. Chen, S. Y. Xie, W. Q. Tian, V. Meunier, S. Zhang, X.-B. Li, *npj Comput. Mater.* **2019**, *5*, 8.

[24] F. Zhang, C. L. Kane, *Phys. Rev. Lett.* **2014**, *113*, 036401.

[25] J. Maciejko, C. Liu, Y. Oreg, X. L. Qi, C. Wu, *Phys. Rev. Lett.* **2009**, *102*, 256803.

[26] S. Heedt, N. Traverso Ziani, F. Crépin, W. Prost, S. Trellenkamp, J. Schubert, D. Grützmacher, B. Trauzettel, *Nat. Phys.* **2017**, *13*, 563.

[27] K. Momma, F. Izumi, *J. Appl. Crystallogr.* **2011**, *44*, 1272.